Anomaly in structural noncentrosymmetry around T_N in bulk and nanoscale BiFeO$_3$

Sudipta Goswami and Dipten Bhattacharya
Nanostructured Materials Division, CSIR-Central Glass and Ceramic Research Institute, Kolkata 700032, India

Gail N. Iles
Department of Crystallography, Helmholtz-Zentrum Berlin, 14109 Berlin, Germany

Barnali Ghosh
Department of Materials Science, S.N. Bose National Center for Basic Sciences, Kolkata 700098, India

Anastasiia A. Prytuliak and Benoit Malard
Science Division, Institut Laue-Langevin, BP 156, 38042 Grenoble, France

Gopes C. Das
School of Materials Science, Jadavpur University, Kolkata 700032, India

B. Ouladdiaf and T. Chatterji
Science Division, Institut Laue-Langevin, B.P. 156, Grenoble 38042, France

Using high resolution powder neutron diffraction data, we show that there is a distinct anomaly in the structural noncentrosymmetry around the magnetic transition point T_N for bulk and nanoscale BiFeO$_3$. It appears that the structural noncentrosymmetry - which gives rise to the ferroelectric polarization - is suppressed anomalously by ~1% (of the average noncentrosymmetry at above the magnetic transition) in the bulk sample and by ~12% in the nanoscale sample as the magnetic transition is approached from higher temperature. This observation shows that the multiferroic coupling improves in the nanoscale sample which is expected to brighten the application prospects of nanoscale BiFeO$_3$ in nanospintronics-based sensor devices.

Key words: multiferroics, structural noncentrosymmetry, powder neutron diffraction, nanoscale BiFeO$_3$

I. INTRODUCTION

In recent times, clear evidence of strong multiferroic coupling at room temperature has been obtained in a single crystal of $BiFeO_3$ in a seminal work (Lebeugle *et al.*, 2008). However, whether the ferroelectric order and multiferroic coupling survive in a nanoscale system has not been clearly determined. The results available in the literature are controversial. While direct determination of ferroelectric domain structure and its switching by piezoforce microscopy (PFM) offers strong evidence of the presence of ferroelectric order in a thin film of just ~2 nm thickness (Chu *et al.*, 2007), results of synchrotron X-ray diffraction, on the other hand, show a melting of the Bi-sublattice even at a size limit of ~18 nm (Petkov, 2010). Likewise, while powder neutron diffraction under 5T magnetic field at room temperature yields evidence of suppression of polarization by ~7% (Goswami *et al.*, 2011b), X-ray diffraction on a sample of comparable particle size does not show any clear signature of multiferroic coupling (Selbach *et al.*, 2008). Therefore, a careful experiment appears to be essential in establishing the survival of ferroelectric order and multiferroic coupling in nanoscale $BiFeO_3$. In this paper, we show, with the help of systematic laboratory X-ray, synchrotron X-ray, and powder neutron diffraction data, that indeed multiferroic coupling survives and even improves in the nanoscale $BiFeO_3$. We report our observation of a clear anomaly in the structural noncentrosymmetry versus temperature plot around the magnetic transition point T_N for both the bulk and the nanoscale $BiFeO_3$. The extent of the anomaly increases at the nanoscale.

II. EXPERIMENTAL

The precursor powder for bulk and nanoscale $BiFeO_3$ was synthesized by solution chemistry route (Goswami *et al.*, 2011a). The powder was compacted and sintered at 830^oC for 5h to prepare the bulk sample. The nanosized particles (of average size ~22 nm) were synthesized by heat-treatment at 450^oC for 2h. The samples have been characterized by laboratory X-ray diffraction, scanning electron and transmission electron microscopy. The representative SEM image of the bulk sample is shown in Figure 1a while the TEM image for the nanosized particles is shown in Figure 1b. The high-resolution TEM image, shown in Figure 1c, shows the nanosized particles to be single crystalline. The magnetic measurement has been carried out across 300-800 K in order to determine the magnetic transition points T_N of the samples.
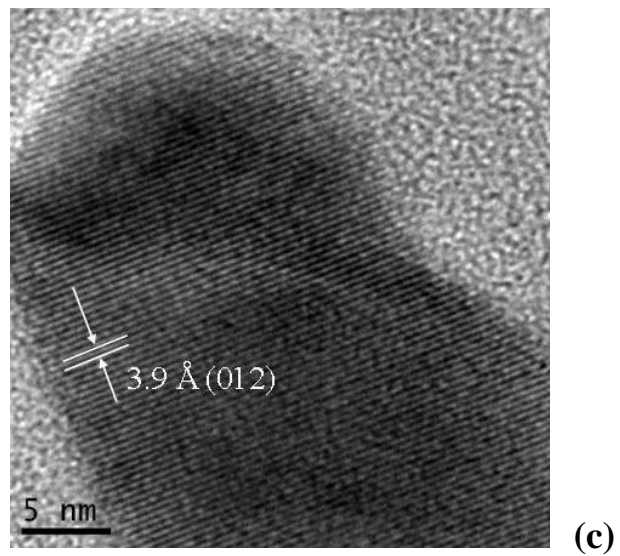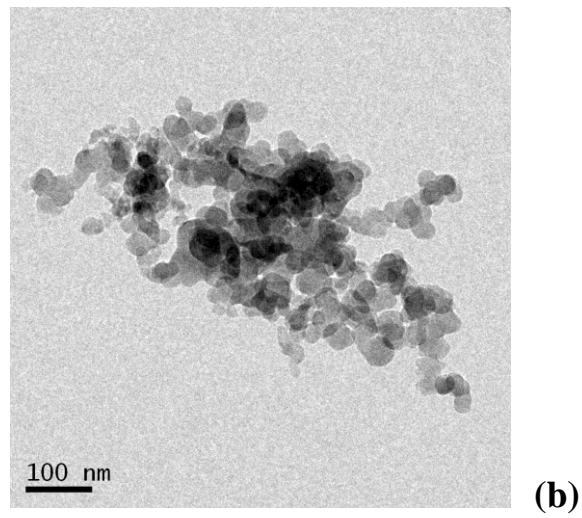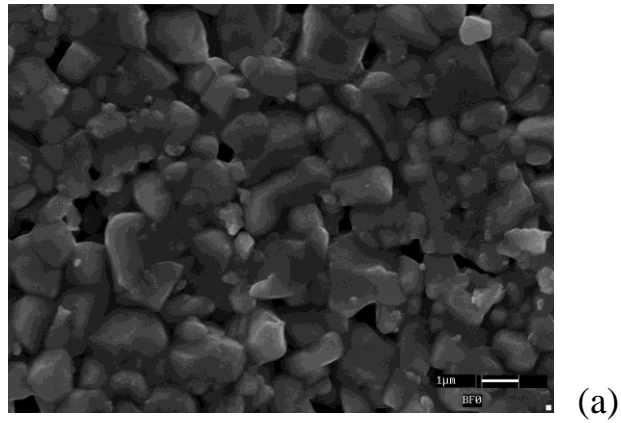
Fig. 1. (a) The scanning electron microscopic image of the bulk sintered pellet of BiFeO$_3$; the average grain size ~0.5 mm; (b) the transmission electron microscopic image of nanoscale particles of BiFeO$_3$; (c) the high resolution transmission electron microscopic image of a nano-sized particle of BiFeO$_3$; the particles are single crystalline with (012) planes perpendicular to beam direction.
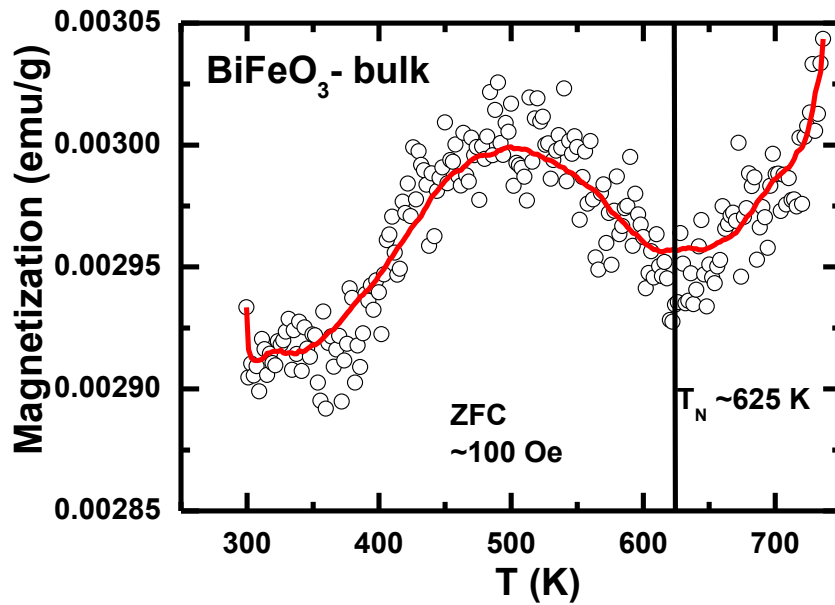
(a)
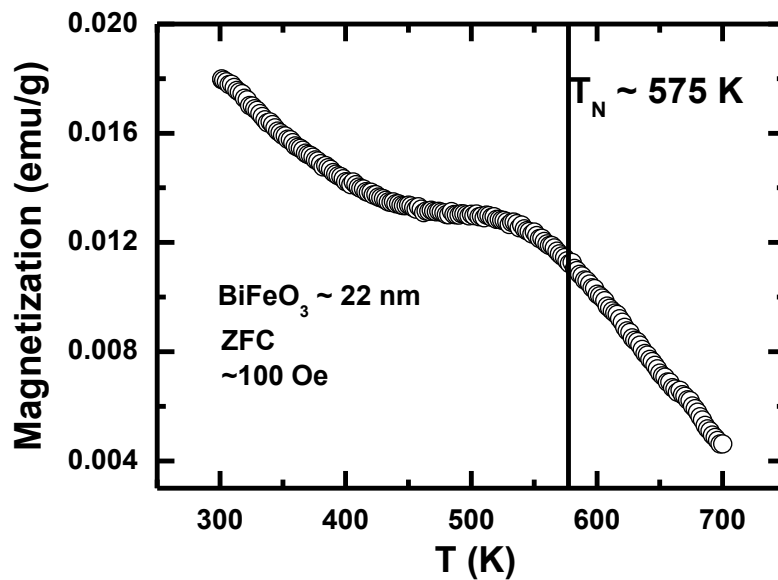
(b)

Fig. 2. (a) The magnetization versus temperature plot for bulk BiFeO$_3$; T$_N$ turns out to be ~625 K with transition width ~50 K; (b) the magnetization versus temperature plot for nanosized particles (~22 nm) of BiFeO$_3$; T$_N$ drops down to ~575 K while transition width increases to ~150 K.

In Figure 2, we show the magnetization versus temperature plot. The T$_N$ appears to have dropped down from ~625 K in bulk to ~575 K in nanoscale particles. The transition width, of course, has increased from ~50 K in the bulk to ~150 K in the nano sample. The broadening of the transition

zone results from distribution in the particle size. The magnetization has increased by nearly a factor of 6 from the bulk to the nanoscale sample. This has been observed (Park *et al.*, 2007) earlier by others as well. It possibly results from an incomplete spin spiral and an increase in the spin canting angle which give rise to a weak ferromagnetism in the nanoscale sample. In order to determine the multiferroic coupling in these samples, laboratory X-ray (Cukα, $\lambda = 1.54060$ Å), synchrotron X-ray $\lambda = 0.3191$ Å), and powder neutron diffraction ($\lambda = 1.748$ Å) patterns have been recorded at several temperatures across the respective T_Ns. The synchrotron data were collected at the ID31 beamline of ESRF, Grenoble whilst the powder neutron diffraction data were recorded at the E9 diffractometer of HZB, Berlin.

III. RESULTS AND DISCUSSION

For determining the accuracy of the atom positions, especially of lighter atoms such as oxygen, estimated from the laboratory and synchrotron X-ray data with respect to that determined from the powder neutron diffraction data, we compared the oxygen positions obtained from these experiments for the bulk $BiFeO_3$. In the supplementary document, we provide the patterns and their refinements as well as the atom positions obtained from the refinement (See supplementary data). The results of the refinement are given in Table-I of the supplementary document.

Table-I: Fit statistics of neutron diffraction data of (a) bulk and (b) nanoscale $BiFeO_3$ at different temperatures.

Bulk

Temperature (K)	B_{ov}	R_p	R_{wp}	χ^2
298	0.105(2)	10.9	10.6	1.05
309	0.113(3)	10.7	12.5	1.95
498	0.152(4)	10.4	10.9	2.05
622	0.225(3)	7.51	11.2	2.25
632	0.256(4)	7.41	11.8	2.47
642	0.289(2)	7.31	11.5	2.35
652	0.286(6)	7.62	11.7	2.40
662	0.295(4)	7.68	11.5	2.32
672	0.308(4)	7.12	11.0	2.10

Nanoscale

Temperature (K)	B_{ov}	R_p	R_{wp}	χ^2
298	0.119(2)	10.8	18.5	2.44
498	0.238(3)	3.93	5.83	6.77
577	0.302(4)	11.2	18.3	2.08
618	0.389(5)	10.9	17.4	1.88
638	0.413(2)	10.4	16.9	2.29
678	0.429(3)	11.5	20.1	2.71
719	0.452(4)	12.8	20.5	2.84
759	0.488(3)	10.9	20.3	2.89
799	0.497(2)	4.50	7.09	2.14

The comparison of the oxygen position - obtained from three different experiments - shows that while O_x and O_z positions determined from synchrotron X-ray and neutron diffraction data are comparable within ~0.5%, the laboratory X-ray data yield a result which differs by ~2-3%. Interestingly, in the case of O_y position, both the laboratory and synchrotron X-ray data yield results comparable within ~0.5% while results obtained from neutron diffraction differs by a staggering ~20%. We have, therefore, restricted ourselves in using powder neutron diffraction data while investigating the structural noncentrosymmetry in bulk and nanoscale $BiFeO_3$. In Fig. 3, we show the representative powder neutron diffraction patterns at several temperatures across the T_Ns and their refinement for both the bulk and the nanoscale samples. The patterns have been refined by FullProf by considering the space group R3c with hexagonal unit cell. The space group does not change from bulk to nanoscale. The propagation vector for the magnetic structure is (0, 0, 0) both for bulk and nanoscale samples.
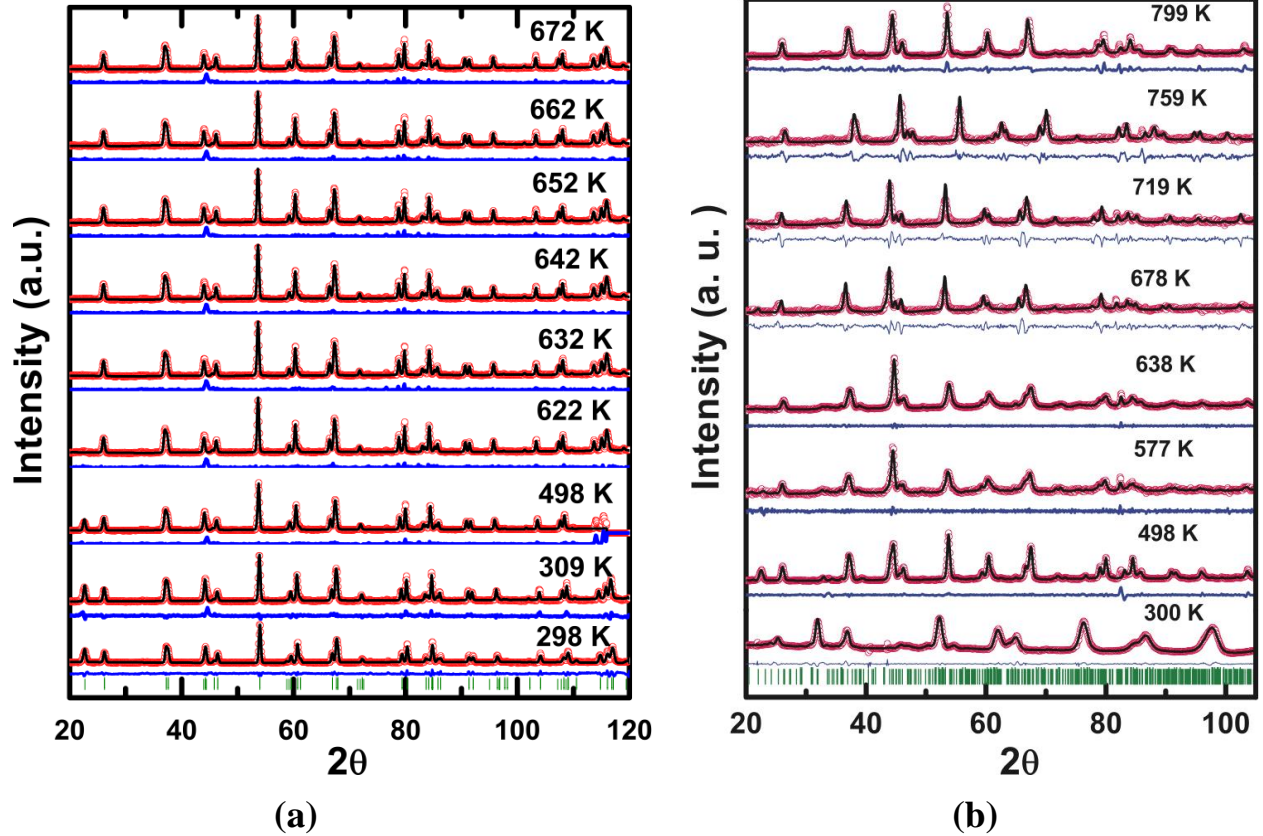
Fig. 3. The powder neutron diffraction data (red circle), fitting (black solid line), difference (solid blue line), and Bragg lines (olive vertical lines) at several temperatures across T_N for (a) bulk and (b) nanoscale $BiFeO_3$.

The fit statistics (R-factors) and the temperature factor B are mentioned in the Table-I. The refinement of the diffraction patterns yields the structural details as well as the magnetic moment per Fe ion in Bohr magneton (m_B). For the bulk sample, the magnetic moment increases from ~3.24(5) m_B/Fe at room temperature to ~3.98(7) m_B/Fe at T_N whereas for the nanoscale sample it is ~3.98(4) m_B/Fe at room temperature and reaches ~4.14(6) μ_B/Fe around T_N and then drops sharply. In Fig. 4, we show the variation of the structural parameters such as lattice volume, bond lengths, and angles across the T_Ns for both the samples. Evidently, in both the cases, all the structural parameters depict clear anomaly around the respective T_Ns.
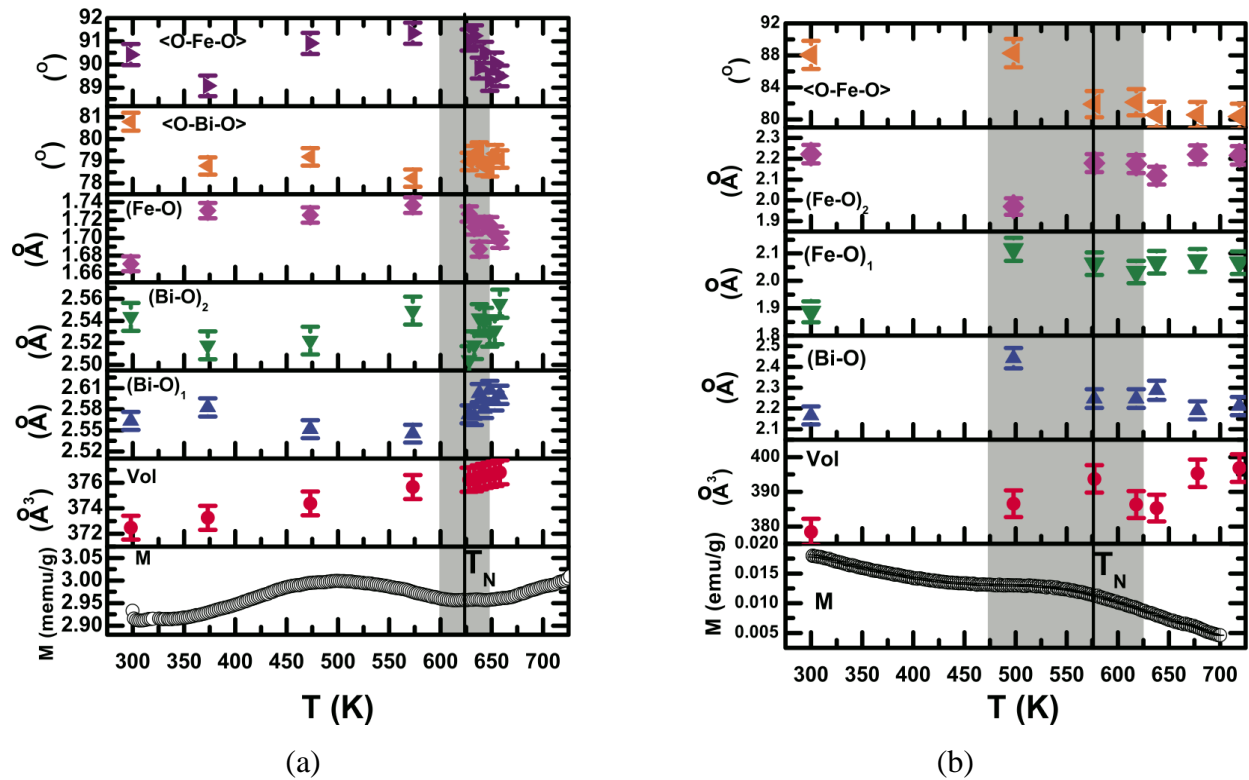
Fig. 4. The magnetization as well as structural parameters such as lattice volume, bond lengths, and angles as a function of temperature determined from the Rietveld refinement of the powder neutron diffraction data for (a) bulk and (b) nanoscale (~22 nm) $BiFeO_3$.

Therefore, onset of magnetic order appears to have influenced the structural parameters significantly. This could result from the magnetoelastic effect. The lattice volume depicts a mere change in slope in variation with temperature across T_N for the bulk sample while a clear volume contraction could be noticed around T_N in the nanoscale sample signifying first order nature of the transition in nanoscale. It is also possible to note that at any given temperature the lattice volume increases from bulk to nanoscale. As far as the variation of bond lengths and angles with temperature is concerned, the following observations could be made: (i) there are two types of Bi-O and Fe-O bonds, respectively, in the bulk and nanoscale samples – long and short; (ii) in the bulk sample, both the Bi-O bonds depict a decrease in length as the T_N is approached from above; (iii) at below T_N the longer Bi-O bond expands gradually while the shorter one first expands sharply and then contracts gradually with the decrease in temperature; (iv) around room temperature the Bi-O bonds start exhibiting a different trend; however, because of lack of data at even lower temperature we could not map out the patterns over this entire temperature range; (v) in the nanoscale sample, on the other hand, both the long and short Fe-O bonds depict a nearly temperature independent patterns at above T_N; (vi) as the T_N is crossed from above, the longer

Fe-O bond first contracts and then expands gradually with the decrease in temperature; (vii) the shorter Fe-O bond expands first and the contracts gradually with the decrease in temperature; (viii) the single bonds – Fe-O in bulk and Bi-O in nanoscale sample – depict an increase in length as the T_N is approached from above; (ix) below T_N while the Fe-O bond length remains nearly temperature independent before decreasing at even lower temperature, the Bi-O bond length decreases gradually; (x) in the bulk sample, the <O-Fe-O> bond angle increases as the T_N is approached from above and then decreases gradually while the trend is just reverse for the <O-Bi-O> bond angle; and finally, (xi) in the nanoscale sample, the <O-Fe-O> bond angle remains nearly temperature independent at above T_N and increases at T_N and then again becomes nearly temperature independent at lower temperature. Apart from the anomaly at T_N for all these parameters, there appears to be a significant anisotropy in the striction effect both in the bulk and the nanoscale sample.

The off-centre displacement (Δd) has also been calculated by noting the difference between the centres of positive and negative charges in a unit cell (Selbach *et al.*, 2008). The plot of Δd as a function of temperature is shown in Fig. 5. *This is the central result of this paper.* For both the bulk and the nanoscale samples, a clear anomaly could be seen around the magnetic transition points. The off-centre displacement appears to have been suppressed at the onset of magnetic order around T_N. For the bulk sample, the suppression turns out to be ~1% of the average off-centre displacement (Δd_{avg}) observed above the magnetic transition. In nanoscale sample it shots up to ~12%. The Δd_{avg} has been calculated by taking an average of the Δd at different temperatures above the magnetic transition for both the samples. Earlier X-ray diffraction data by others did not show any clear anomaly in the off-centre displacement around T_N even for a bulk sample (Selbach *et al.*, 2008). Therefore, it appears that the high resolution powder neutron diffraction data are more useful in determining the position of the oxygen ions and hence the off-centre displacement in a cell accurately.
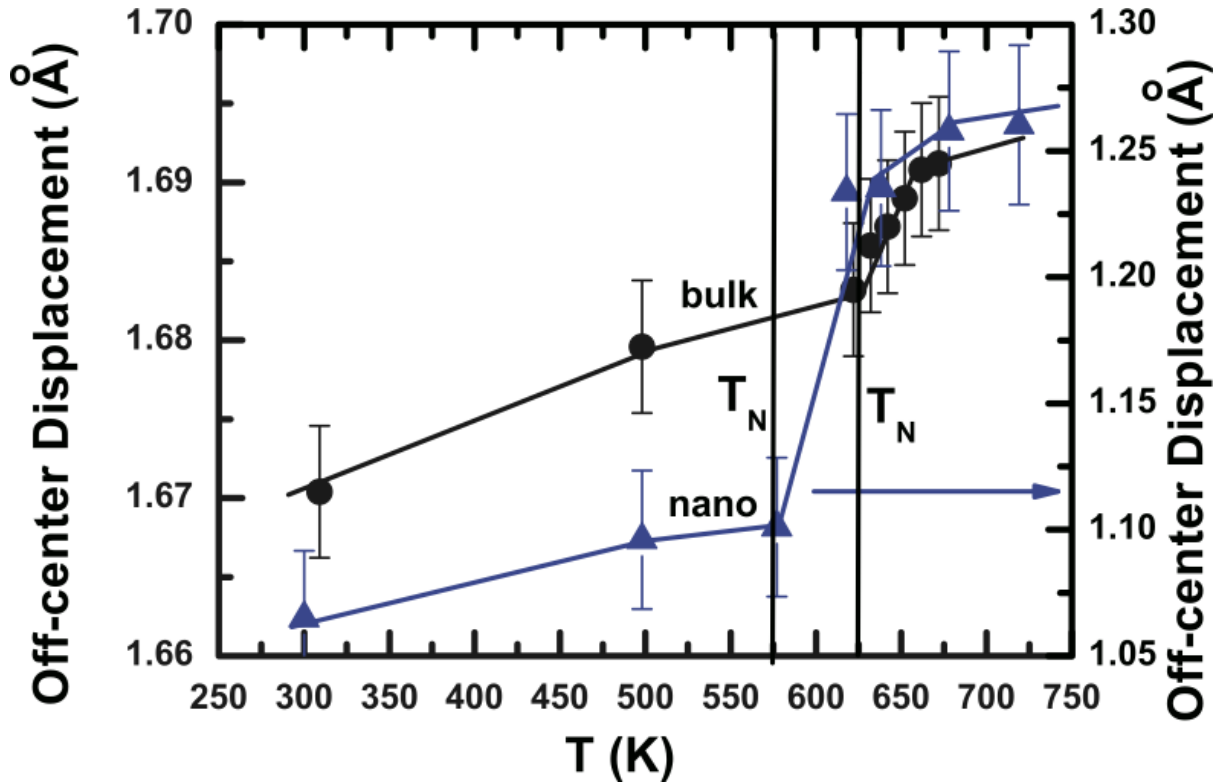
Fig. 5. The anomaly in noncentrosymmetry around T_N both for bulk and nanoscale $BiFeO_3$.

Because of antiferromagnetic spin cycloid in bulk $BiFeO_3$, it was predicted that the linear multiferroic coupling could be nearly zero (Tabarez-Munoz *et al.*, 1985). Indeed, the polycrystalline samples investigated in the past did not depict a strong coupling (Popov *et al.*, 1993). However, in a single crystal of $BiFeO_3$ one observes a very strong coupling (Lebeugle *et al*., 2008). The origin of this strong multiferroic coupling in bulk $BiFeO_3$ appears to lie in the coupling between polarization resulting from the spin cycloid (Mostovoy *et al.*, 2006) and that from the polar domains. In the nanoscale sample of size smaller than 62 nm, the spin cycloid becomes incomplete and hence one should observe a weak coupling. However, it has been noted already (Park *et al.*, 2007) that incomplete spin spiral gives rise to a weak ferromagnetism and hence larger magnetization. Large magnetization is associated with the rotation of nonferroelectric oxygen octahedra around the [111] axis via the Dzialoshinskii-Moriya exchange interaction (Ederer *et al.*, 2005). This rotation, in turn, is coupled with the rotation of the polar domains. Therefore, enhanced magnetization could give rise to an enhanced multiferroic coupling.

Improved multiferroic coupling in nanoscale (~22 nm) $BiFeO_3$ brightens the prospect of using this system in nanospintronics-based devices. It remains to be seen, however, whether the multiferroic coupling keeps improving as the size is reduced even further or does it decrease because of fluctuations in the magnetic and ferroelectric domain structures. The optimum size limit at which the multiferroic coupling maximizes in $BiFeO_3$ needs to be determined and is a future challenge.

IV. SUMMARY

In summary, we report here that from high resolution powder neutron diffraction data, we could see a clear anomaly in off-centre displacement around the magnetic transition point T_N for both bulk and nanoscale (~22 nm) $BiFeO_3$. This was not observed earlier from the X-ray diffraction data. The extent of the anomaly, i.e., suppression of polarization at the onset of magnetic order increases from ~1% in bulk to ~12% in nanoscale. The percentage is of the average noncentrosymmetry observed at above T_N. The coupling between the spin cycloid driven polarization and the polarization from polar domains gives rise to the multiferroicity in the bulk system. In the nanoscale system, on the other hand, enhanced magnetization due to suppression of spin spiral leads to an enhanced rotation of nonferroelectric FeO_6 octahedra around the [111] axis. This, in turn, gives rise to the multiferroic coupling observed because of the coupling between the rotation of FeO_6 octahedra and the ferroelectric domains. It remains to be seen whether the coupling improves further or not if the particle size is reduced further.

Supplementary data available

Chu, Y. H., Zhao, T., Cruz, M. P., Zhan, Q., Yang, P. L., Martin, L.W., Huijben, M., Yang, C. H., Zavaliche, F., Zheng, H. and Ramesh, R. (**2007**). "Ferroelectric size effects in multiferroic $BiFeO_3$ thin films," Appl. Phys. Lett. **90**, 252906(1-3).

Ederer, C. and Spaldin, N. A. (**2005**). "Weak ferromagnetism and magnetoelectric coupling in bismuth ferrite," Phys. Rev. B: Condens. Matter Mater. Phys. **71**, 060401.

Goswami, S., Bhattacharya, D. and Choudhury, P. "Particle size dependence of magnetization and noncentrosymmetry in nanoscale $BiFeO_3$," (**2011a**). J. Appl. Phys. **109**, 07D737.

Goswami, S., Bhattacharya, D., Choudhury, P., Ouladdiaf, B. and Chatterji T. (**2011b**). Appl. Phys. Lett. **91**, 073106.

Lebeugle, D., Colson, D., Forget, A., Viret, M., Bataille, A. M. and Gukasov, A. (**2008**). "Electric-field-induced spin flop in $BiFeO_3$ single crystals at room temperature," Phys. Rev. Lett. **100**, 227602.

Mostovoy, M., (**2006**). "Ferroelectricity in spiral magnets," Phys. Rev. Lett. **96**, 067601.

Park, T.-J., Papaefthymiou, G. C., Viescas, A. J., Moodenbaugh, A. R. and Wong, S. S. (**2007**). "Size-dependent magnetic properties of single-crystalline multiferroic $BiFeO_3$," Nano Lett. **7**, 766-772.

Petkov, V., Selbach, S. M., Einarsrud, M.-A., Grande, T. and Shastri, S. D. (**2010**). "Melting of Bi sublattice in nanosized $BiFeO_3$ perovskite by resonant X-ray scattering," Phys. Rev. Lett. **105**, 185501.

Popov, Y. F., Zvezdin, A. K., Vorob'ev, G. P., Kadomtseva, A. M., Murashev, V. A. and Rakov, D. N. (**1993**). "Linear magnetoelectric effect and phase transitions in bismuth ferrite, $BiFeO_3$," JETP Lett. **57**, 69-73.

Selbach, S. M., Tybell, T., Einarsrud, M.-A. and Grande, T. (**2008**). "The ferroic phase transitions of $BiFeO_3$," Adv. Mater. **20**, 3692-3696.

Tabarez-Munoz, C., Rivera, J.-P., Bezinges, A., Monnier, A. and Schmid, H. (**1985**). "Measurement of the quadratic magnetoelectric effect on single crystalline $BiFeO_3$," Jpn. J. Appl. Phys. **24**, 1051-1053.